IJARSCT
ISSN (Online) 2581-9429
International Journal of Advanced Research in Science, Communication and Technology (IJARSCT)
Volume 2, Issue 9, June 2022
Impact Factor: 6.252

Eco-friendly Synthesis, Spectral Characterization, Particle Image and Size Analysis of Cerium Oxide Nanoparticles Mediated by Mango Seed Aqueous Extract

P. Sindhu[1], V. Vinmathi[1], K. Sathiyamoorthi[2], B. Anand[3*]
PG Students, PG & Research Department of Physics[1]
Assistant Professor, PG & Research Department of Chemistry[2]
Assistant Professor, PG & Research Department of Physics[3]
Government Arts College, Chidambaram, Tamil Nadu, India
Corresponding author email:banandphysics@gmail.com

Abstract: *A novel approach for the utilization of fruit waste is attempted in the present investigation. Mangifera indica seed aqueous extract was utilized for green synthesis of cerium oxide nanoparticles (CeONPs). The phyto constituents in the seed acted as reducing and stabilizing agent for CeONPs formation. UV-Vis, FT-IR, FL, XRD, DLS and SEM, analysis were used to characterize the green synthesized CeONPs. UV-vis spectra showed characteristic spectra at 333 nm; DLS and SEM confirmed the crystalline nature. FT-IR revealed functional groups like alcohol or phenols, carboxylic acids, ketones, amines, aromatic amines, aliphatic amines, alkyl halides and alkynes which were responsible for CeONP formation. The nanoparticles showed more CV study of cerium oxide nanoparticle. Fruit waste can be successfully utilized for cerium nanoparticles formation which can be therapeutically useful and effective.*

Keywords: Eco-friendly synthesis, CeONPs, Mangifera indica seed, Spectral characterization and CV study

I. INTRODUCTION

Cerium oxide CeO_2 (CeO_2NPs) crystal lattice, consists of a cerium core enveloped by an oxygen lattice. These particles have an interesting feature, coexistence of Ce^{3+} and Ce^{4+} ions and the ability of oxygen vacancies formation on their surface, which enables them to interact with and modulate free radicals. In such way these nanoparticles can pass many cycles of reactions with free radicals and thus regenerate themselves in every cycle [1,2]. This is a unique feature making CeO_2NPs advantageous in comparison with the other nanoparticles. Besides, compared with other rare earth elements, CeO_2NPs have a high hydrogen-absorbing capacity, such that reactions with H_2, O_2, or H_2O occur more readily, which may account for its regenerative capacity as a catalyst [3]. As such, they display antioxidant/antiradical activity [4,5] that encouraged studies of pharmacological potential of these nanoparticles, as well as their biomedical applications [6–8]. Some studies have shown protective effect of the CeO_2NPs towards oxidant-mediated apoptosis [9,10]. However, in certain studies CeO_2NPs induced oxidative stress either in vitro or in vivo [11,12]. CeO_2 nanoparticles (NPs) have received much attention in nanotechnology due to their useful applications as catalysts, fuel cells and antioxidants in biological systems.[13-17] In general; cerium can exist in two oxidation states: Ce^{3+} and Ce^{4+}. Therefore, cerium dioxide can have two different oxide forms, CeO_2 (Ce^{4+}) or Ce_2O_3 (Ce^{3+}), in bulk material[18] On the nanoscale, the cerium oxide lattice has a cubic fluorite structure, and both Ce^{3+} and Ce^{4+} can coexist on its surface. Charge deficiency due to the presence of Ce^{3+} is compensated by oxygen vacancy in the lattice; thus, CeO_2-NPs contain intrinsic oxygen defects.[19] these oxygen defects are actually sites of catalytic reactions. The concentration of oxygen defects increases with reduction in particle size.[20] Therefore; CeO_2-NPs have improved redox properties with respect to the bulk materials. Moreover, the presence of a mixed valance state plays an important role in scavenging reactive oxygen and nitrogen species. CeO_2-NPs are found to be effective against pathologies associated with chronic oxidative stress and inflammation. Recently, CeO_2-NPs have also been reported to have multienzyme, including superoxide oxidase, catalase and oxidase, and mimetic properties, and have emerged as a fascinating material in biological fields, such as in bioanalysis, [21-25] biomedicine15 and drug delivery.[26-27] These applications are derived from quick transition of the oxidation state between Ce^{3+} and Ce^{4+}. The surface Ce^{3+}:Ce^{4+} ratio is influenced by the microenvironment. Therefore, the microenvironment and synthesis method adopted also plays an important role in determining the biological activity and toxicity of CeO2-NPs. The CeO_2-

IJARSCT
ISSN (Online) 2581-9429
International Journal of Advanced Research in Science, Communication and Technology (IJARSCT)
Volume 2, Issue 9, June 2022
Impact Factor: 6.252

NPs have been prepared through the means of several routes and synthesis methods including solution precipitation,[28] sonochemical,[29] hydrothermal,[30] solvothermal,[31] ball milling,[32] thermal decomposition,[33] spray pyrolysis,[34] thermal hydrolysis25 and sol–gel methods.26–28 However, applying the mentioned methods deals with several drawbacks, such as toxic solvents and reagents usage, high temperature and pressure, and the requirement of external additives as stabilizing or capping agents during the reaction. As the physiochemical properties of NPs mostly depend on the synthesis procedure, the synthesis method of NPs for biological applications is very important. The physical properties (size, surface charge, agglomeration status in liquid and coating or residual contamination of the surfactant on the surface) of NPs mainly influence interactions at the nano–bio interface. Moreover, the surface Ce^{3+}:Ce^{4+} ratio (chemical property) also influences the biocatalysis and the biological interactions. Manipulation of the surface Ce^{3+}:Ce^{4+} ratio can be achieved by controlling their synthesis method. However, coating the NPs with biocompatible/organic polymers increases dispersion/stability, decreases nonspecific interactions with cells and proteins, increases blood circulation time and reduces the toxicity of the NPs.

2. MATERIAL AND METHODS

2.1. Collection of Sample

The seed of M. indica were collected from my home kitchen waste. The seeds were manually separated after breaking seed kernel, shade dried at room temperature and homogenised to fine powder and stored in air tight bottles

2.2. Chemicals, Solvents and Starting Materials

All the metal salts and de-ionized water, whatmann 1≠ and whatmann 41≠ filter papers, Ethyl alcohol, sodium hydroxide pellets, Hydrochloric acids, sulphuric acid and other chemicals were purchased from Merck (India) Ltd. All chemicals were used without further purification.

2.3 Instruments and equipment

Electric oven, Magnetic stirrer (REMI 2 MLH), E-1 portable TDS & EC meter, pH-009(I)A pen type pH meter, sterilized 250ml separating funnels, sterilized conical flasks, sterilized 400ml beakers, watch glasses, 7'' funnels, glass rods, and 10ml measuring cylinders,

2.4. Preparation of *Mangifera indica* (mango) Seed Extract

5 grams of powdered *Mangifera indica* (mango) seed with 50 mL of double-distilled water (DDW) taken in the 250 mL round bottomed flask, water condenser fitted and fix the running tap water then heated for 20 min at 80^{O} C. Then the extract was filtered with Whatmann 1≠ filter paper. The filtrate was used to the further green synthesis of process

Figure 1: Green synthesis of Cerium oxide nanoparticles mediated by Mango seed kernel extract

2.5 Synthesis of Cerium Oxide Nanoparticles (CeONPs)

Synthesis of CeNPs was carried out by reducing Cerium ammonium sulphate (M.F: $(NH_4)_4$ $(SO_4)_2$. $Ce(SO_4)_2$, MW: 632.55 g/mol) using *Mangifera indica* (mango) seed extract. To achieve this purpose, 100 mL of saturated solution of Cerium ammonium sulphate is steadily mixed with 10mL of *Mangifera indica* (mango) seed extract, immediately

IJARSCT
ISSN (Online) 2581-9429
International Journal of Advanced Research in Science, Communication and Technology (IJARSCT)
Volume 2, Issue 9, June 2022
Impact Factor: 6.252

obtained milky colour colloidal suspensions [35]. The colour of the solution is turn in Pale golden-yellowish solution turn to milky white (**Fig:1**). Further, obtained suspension filtered with wattman 1≠ filer paper . Supernatant was discarded and pellet containing CeNPs was carefully washed 3 times with distilled water to remove uncoordinated materials. The obtained powder assumed as CeNPs was incubated at ~100 °C until the water evaporated completely. Finally, CeONPs were thoroughly characterized.

III. CHARACTERIZATION

The absorption maximum of the cerium oxide nanoparticles was measured by ultraviolet spectrum. The FTIR spectrum was recorded on Nicolet IS10 (Thermo Scientific, Waltham, MA) at room temperature. The IR spectrum was noted in the range of 400–4000 cm^{-1}. Different modes of vibrations were identified and assigned to determine the different functional groups present in the cerium oxide nanoparticles by M. indica seed extract. Another one spectral studies carried out by fluoresce spectroscopy. DLS Ananlysis was used to measure the average size of the green synthesized nanoparticles, SEM analysis was done to visualise the shape as well as to measure the diameter of the green synthesized CeONPs. And additionally measured the reduction potential of the cerium oxide nanoparticles by cyclic voltmeter studies.

IV. RESULT AND DISCUSSION

4.1 UV-Vis Spectral Analysis

UV-visible spectroscopy is one of the most widely used techniques for structural characterization of CeNPs. **Figure 2,** shows the UV-Vis spectra of obtained CeNPs mediated by Extract of red rose petal. SPR band was broad, indicating poly-dispersed nanoparticles. SPR band around 333 nm broadened and slightly moved to the long wavelength region indicating the presence and formation of CeNPs. The optical absorption spectra of metal NPs were dominated by SPR, which shift to longer wavelengths with increasing particle size. The position and shape of plasmon absorption of cerium nanoparticles were strongly dependent on the particle size, dielectric medium and surface-adsorbed species. The surface Plasmon absorption of CeNPs has the short wavelength band in the visible region around 333 nm due to the transverse electronic oscillation

4.2 FT-IR spectral Analysis

The FTIR analysis was further performed to determine the phyto-constituent containing functional groups involved in synthesizing Ce_4O_8 nanoparticles as reducing and capping agents. **Figure:3** presented the FTIR spectrum of cerium nanoparticle by mango seed extract. The results of CeONPs FTIR spectrum demonstrated that the frequency of 3425 cm^{-1} at the very broad peak represent the various stretching frequencies are merged to appeared it, this peak had been screened out -O-H group in alcohols and acids, the peak of 2924 demonstrate CH_3, CH_2 & CH 2 or 3 bands, The sharp stretching frequency of 1632 cm^{-1} have represented by -C=O- group contain functional groups of aldehyde, acid and its derivatives. -N-H group in amide, -C=N nitrile, -C-H aromatic stretching and aldehydic –CH stretching frequencies, frequency of 1384 cm^{-1} is represent in N-H bending) , the peak of 606 cm^{-1} have shown in Ce-O stretching vibrations. These results suggest that many biologically active phyto-molecules are left adsorbed on the surface of the Ce_4O_8 nanoparticles

4.3 Fluorescence Spectral Analysis

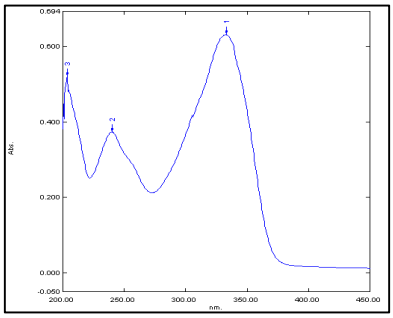

Fig:3 UV spectrum of CeONPs

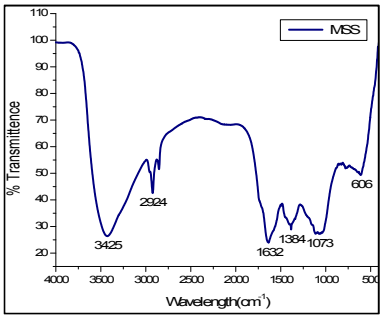

Fig:4 FTIR Spectrum of CeONPs

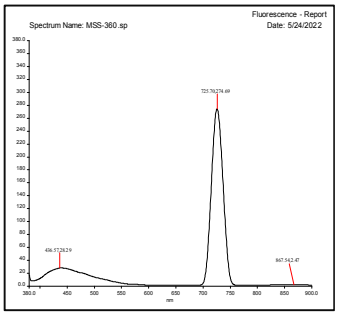

Fig:4 FL Spectrum of CeONPs

IJARSCT
ISSN (Online) 2581-9429
International Journal of Advanced Research in Science, Communication and Technology (IJARSCT)
Volume 2, Issue 9, June 2022
Impact Factor: 6.252

The fluorescence emission spectrum has been shown an obvious peak at 725.70 nm in CeONPs by mango seed extract sample, shows no trend in neither the Stern-Volmer quenching plot nor the direct fluorescence method **(Figure4**). Overall, even in the presence of CeONPs nanoparticles.

4.4 DLS Analysis

DLS is often interpreted to as a scattering of quasi-elastic light. It fulfills the role of size distribution and agglomeration of selective NPs (**Fig:5**). This process is quite sensitive, rapid and it can calculate the mean size of a particle on both macro and nano scale. The speed of the DLS technique is based on particle size. Small particles in suspension undergo random thermal motion known as Brownian motion. This random motion is modeled by the Stokes-Einstein equation. Below the equation is given in the form most often used for particle size analysis. The DLS analysis of green synthesized cobalt nanoparticle to shown the average size of the nanoparticle is 94.08 nm. This result also shown in some of the nanoparticle having more than 100 nm, this is due to growth of the nanoparticle and aggregation of the two is more nanoparticles.

4.5 SEM Analysis

The morphology determined by SEM analysis of green synthesized Ce_3O_4 nanoparticle by rose petal aqueous extract has shown **Figure;6**. It can be seen from SEM image that Ce_3O_4NPs are agglomerated and not well formed. One can vividly see well defined nanoparticles with distinguish shapes. Specifically, SEM image for Ce_3O_4NPs reveal distinguishable rhomboid shaped nanoparticles, elongated nano bead and highly agglomerated nanoparticles, Ce_3O_4 nanoparticles become well-formed reveling distinct shapes. SEM image of cerium oxide nanoparticles are rocky shaped and very fine and sharp broken rock shaped. To identify chemical elements and purity of synthesized samples.

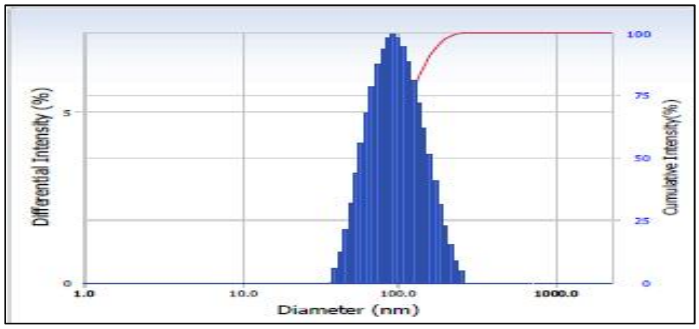

Figure 5: DLS spectrum of Cerium oxide nanoparticles.

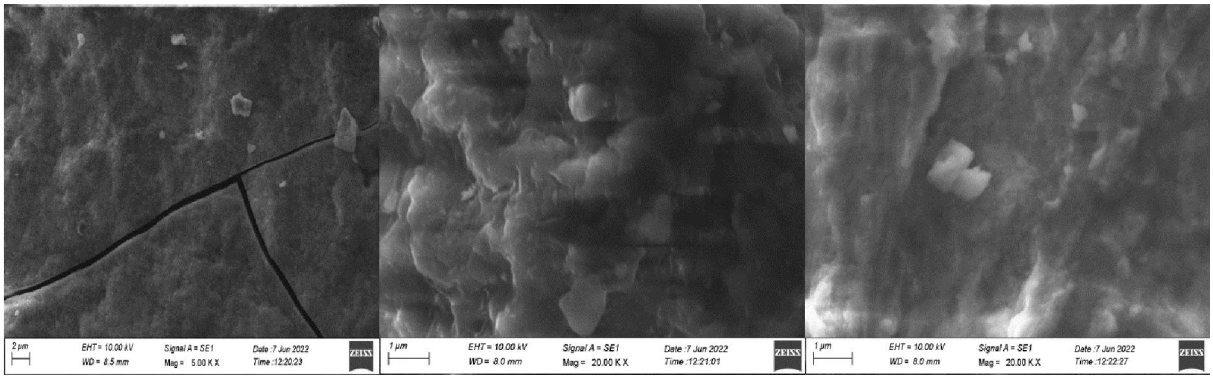

Figure 6: SEM Images of Cerium oxude nanoparticles by mango seed extract

IJARSCT
ISSN (Online) 2581-9429
International Journal of Advanced Research in Science, Communication and Technology (IJARSCT)
Volume 2, Issue 9, June 2022
Impact Factor: 6.252

4.6. Cyclic Voltammetry and Discharge Curve

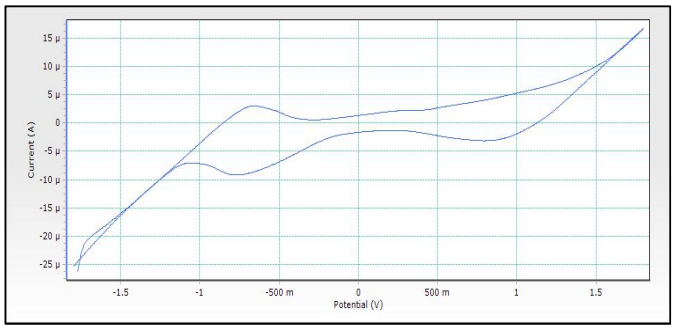

Figure 6: CV spectrum of cerium oxide nanoparticle by mango seed extract

The shape of the cyclic voltammetry curves is an ideal rectangular shape observed at 10 mV/s. Further increasing the scan rate the observed pattern of the CV curve is altered and it confirms the pseudo capacitive nature of the material**.** The specific capacitance (SC) values of manganese ferrite electrode can be estimated by using the formula

$$Cs = Q / m\Delta V$$

Where, Cs is the specific capacitance, Q the anodic and cathodic charges on each scanning, m is the mass of the electrode material (mg) and ΔV is the scan rate (mVs^{-1}). Electrochemical measurements were performed in 0.2 tetra butyl ammonium perchlorate with a standard three electrode configuration consisting of a sample (working electrode), an Ag/ AgCl (reference electrode) and a high platinum wire (counter electrode). The scan rate increased in the range from 10 mV/s to 100mV/s and its corresponding specific capacitance values depicted in Fig.15 Further, the specific capacitance values of 290.4 F/g observed in the scan rate of 10 mV/s for the sample annealed at 700°C. The reason for high specific capacitance at low scan rate is observed in the present study suggested that the ionic diffusion takes place both inner and outer surfaces. The higher specific capacitance values observed in the present study confirm the good crystalinity of the cerium nanoparticles.

V. CONCLUSION

In the present work, in accordance with the saying best from waste, we have synthesized CeONPs from M. indica fruit waste i.e. seed. The phytochemicals in the seed acted as reducing and stabilizing agent for the formation of CeONPs. The green synthesized nanoparticles were round or spherical in shape with an average size of 94.08 nm. This is a good example of best from waste. Seeds which are generally discarded as waste into the environment can be used to synthesize CeONPs which can be therapeutically used to control many diseases especially infectious, stress related and cancer. They can be a good source of natural antimicrobial, antioxidant and anticancer agents. Further work in understanding the molecular mechanism and in vivo studies are needed. Work in this direction is in progress

REFERENCES

[1]. H. Mirzaei and M. Darroudi, Ceramics International, 43. 1, (2017) 907–914.
[2]. S. C. C. Arruda, A. L. D. Silva, R. M. Galazzi, R. A. Azevedo, and M. A. Z. Arruda, "Nanoparticles applied to plant science: a review," Talanta,131(2015) 693–705.
[3]. H. Agarwal, S. V. Kumar, and S. Rajeshkumar, "Rsource- Efficient Technologies., 3, 4 (2017) 406–413.
[4]. H. A. Salam, R. Sivaraj, and R. Venckatesh, Materials Letters, vol. 131, pp. 16–18, 2014.
[5]. P. T. Anastas and J. C. Warner, Green Chemistry: Theory and Practice, Oxford University Press, Oxford, UK, 2000.
[6]. W. Cai and X. Chen, "Nanoplatforms for targeted molecular imaging in living subjects," Small., 3, 11 (2007) 1840–1854.
[7]. H. Hong, Y. Zhang, J. Sun, and W. Cai, "Nano Today., 4, 5 (2009) 399–413.
[8]. Y. Zhang, H. Hong, D. V. Myklejord, and W. Cai, Small., 7, 23(2011) 3261–3269.
[9]. M. V. Yigit and Z. Medarova American Journal of Nuclear Medicine and Molecular Imaging, 2, 2,(2012) 232–241.
[10]. J. E. Hutchison., ACS Nano., 2, 3 (2008) 395–402.

IJARSCT
ISSN (Online) 2581-9429
International Journal of Advanced Research in Science, Communication and Technology (IJARSCT)
Volume 2, Issue 9, June 2022
Impact Factor: 6.252

[11]. W. Cai, A. R. Hsu, Z.-B. Li, and X. Chen, "Nanoscale Research Letters, vol. 2, 6 (2007) 265–281.
[12]. W. Cai and H. Hong, "In a American Journal of Nuclear Medicine and Molecular Imaging, 2, 2 (2012)136–140.
[13]. L. R. Hirsch, A. M. Gobin, A. R. Lowery et al., "Metal nanoshells," Annals of Biomedical Engineering, 34,1 (2006) 15–22.
[14]. L. Lacerda, A. Bianco, M. Prato, and K. Kostarelos, Advanced Drug Delivery Reviews, 58, 14(2006)1460–1470.
[15]. H. Hong, T. Gao, and W. Cai, Nano Today, 4, 3 (2009) 252–261.
[16]. Z. L. Wang, ACS Nano, 2, 10 (2008) 1987–1992.
[17]. P. Yang, R. Yan, and M. Fardy, Nano Letters, 10, 5 (2010)1529–1536.
[18]. M. H. Huang, Y. Wu, H. Feick, N. Tran, E. Weber, and P. Yang, Advanced Materials, 13, 2 (2001)113–116.
[19]. Z. Fan and J. G. Lu, Jr of Nanoscience and Nanotechnology., 5,10 (2005)1561–1573.
[20]. C. S. Lao, M.-C. Park, Q. Kuang et al., Journal of the American Chemical Society, 129, 40 (2007) 12096-12097.
[21]. X. Wang, J. Liu, J. Song, and Z. L. Wang, Nano Letters., 7, 8 (2007) 2475–2479.
[22]. Y. Yang, W. Guo, Y. Zhang, Y. Ding, X. Wang, and Z. L. Wang, Nano Letters, 11, 11(2011) 4812–4817.
[23]. R. Yakimova, Frontiers in Bioscience, 4, 1(2012) 254–278.
[24]. J. Zhou, N. S. Xu, and Z. L. Wang, Advanced Materials, 18, 18 (2006) 2432–2435.
[25]. Y. Zhang, T. Nayak, H. Hong, and W. Cai, Current Molecular Medicine, 13, 10 (2013) 1633–1645.
[26]. M. Pandurangan and D. H. Kim, Journal of Nanoparticle Research., 17, 3 (2015)158.
[27]. V. N. Kalpana and V. D. Rajeswari, Food Biosynthesis, (2017) 293–316.
[28]. A. Bose, Emerging Trends of Nanotechnology in Pharmacy, Pharmainfo, 2016,
[29]. A. Alagarasi, Introduction to Nanomaterials, National Centre for Catalysis Research, Chennai, India, 2011, https://nccr.iitm.ac.in/2011.pdf.
[30]. V. Thirumalai Arasu, D. Prabhu, and M. Soniya, Journal of Biosciences Research, 1 (2010) 259–270.
[31]. G. Rajakumar, T. Gomathi, M. Thiruvengadam, V. D. Rajeswari, V. N. Kalpana, and I. M. Chung, Microbial Pathogenesis, 103 (2017) 123–128.
[32]. P. Raveendran, J. Fu, and S. L. Wallen, Journal of the American Chemical Society, 125, 46 (2003)13940-13941.
[33]. P. Dhandapani, S. Maruthamuthu, and G. Rajagopal, Journal of Photochemistry and Photobiology B: Biology, vol. 110, pp. 43–49, 2012.
[34]. F. Zhang, P. Wang, J. Koberstein, S. Khalid, S.W. Chan, Surf. Sci. 563 (2004) 74–82.
[35]. A.S. Karakoti, N.A. Monteiro-Riviere, R. Aggarwal, J.P. Davis, R.J. Narayan, W.T. Self, J. McGinnis, and S. Seal., Nanoceria as Antioxidant: Synthesis and Biomedical Applications JOM (1989).: JOM (1989). 2008 Mar 1; 60(3): 33–37